CIRP Annals - Manufacturing Technology xxx (2015) xxx–xxx

Contents lists available at ScienceDirect

CIRP Annals - Manufacturing Technology

journal homepage: http://ees.elsevier.com/cirp/default.asp

Material removal mechanism in low-energy micro-EDM process

Jun Qian *, Fei Yang, Jun Wang, Bert Lauwers (1), Dominiek Reynaerts

Department of Mechanical Engineering, KU Leuven, Leuven, Belgium

ARTICLE INFO

Keywords:
Electrical discharge machining (EDM)
Material removal mechanism
Negative current flow

ABSTRACT

Extensive experiments have been carried out to understand the fundamentals in micro-EDM and especially the material removal mechanism in the finishing regimes of micro-EDM with a RC type generator. Oscillation of the sparking current and voltage has been observed when a high open-voltage was applied and this phenomenon has been predicted by electrical simulations and further experimentally verified. Experiments show that the effect of negative current flow in the sparking gap is not a simple polarity switch. Contrary to the conventional understanding, the negative current flow in a single sparking cycle is also contributing to effective material removal on the workpiece.

1. Introduction

Electro-discharge machining (EDM) is one of the effective manufacturing technologies for electrically conductive or semi-conductive hard materials [1–3]. There are basically two kinds of generators utilized in an EDM system, either an RC type generator [4] or a transistor type generator [5,6]. In micro EDM applications, an RC relaxation type generator is usually adopted in order to obtain a low sparking energy for small volumetric material removal per discharge [6–8]. Fig. 1 illustrates the basic diagram of a micro-EDM machine, in which the power generator consists of a voltage source U supplying a constant or pulsed DC voltage, a charging resistor R, and a charging capacitor C_e. The cable connection is modelled as a parasitic inductance L_p and resistance R_p in series. The sparking gap model includes two parts connected in parallel: an equivalent parasitic capacitor of the discharge gap and the discharge cable C_p, and a voltage source which models the plasma channel after the gap breakdown [1]. Depending on the length of the cable that is used, L_p and R_p will eventually not be negligible.

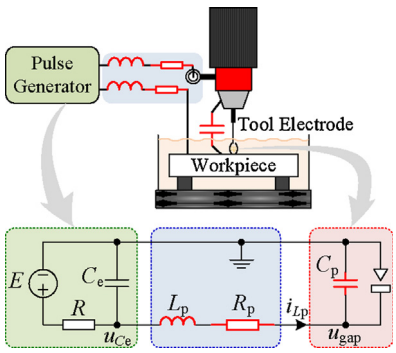

Fig. 1. Schematic of RC electrical circuit micro-EDM.

After a normal discharge, due to the voltage difference between u_{Ce} and u_{gap} and the tank circuit composed of L_p, C_e and C_p, u_{gap} will resonate with a large amplitude and relatively high frequency. Within a short period after a normal discharge, there is insufficient time to neutralize the sparking gap. With the high negative voltage and the debris remained in the gap, it is possible that the gap breakdown occurs under the reversed polarity. Even multiple discharges can occur alternatively in both polarities [7,9] and this results in influence on uncertainty of discharge energy [8]. During experiments on two micro-EDM devices (AGIE® Compact 1 and Sarix® SX-100-HPM) at low energy settings, in "negative" polarity connection and with tungsten carbide as the tool electrode and stainless steel as the workpiece, there have been observations of negative current and voltage with a low open voltage, e.g. 100 V, in Fig. 2(a) and alternating current and voltage flow at a high open voltage of 160 V in Fig. 2(b), respectively. As seen in Fig. 2, except for the much short ignition time and polarity, the voltage and current forms of the following waves are similar to those of the first normal discharge. The voltage peak in both polarities is nearly on the same level and the current gradually decays due to the energy dissipation.

Different from the existing understanding that the plasma channel is closed once the sparking current reaches zero [10], it can be hypothesized from the observations above that the plasma channel remains open after the first discharge. The objectives of this paper are twofold: understanding the phenomena of the sparking with alternating voltage and current flow observed in the micro-EDM process with a RC type generator on one hand, and their influences on the machining performance, i.e. material removal rate and tool wear on the other hand.

2. Electrical-circuit based simulation of sparking gap

In spite of the difficulties in directly proving the opening of the gap after the first discharge, it is reasonable to verify the phenomena from an electrical circuit perspective based on the experimental waveforms. Fig. 3(a) depicts the schematics of

* Corresponding author.
E-mail address: jun.qian@kuleuven.be (J. Qian).

http://dx.doi.org/10.1016/j.cirp.2015.04.040
0007-8506/© 2015 CIRP.

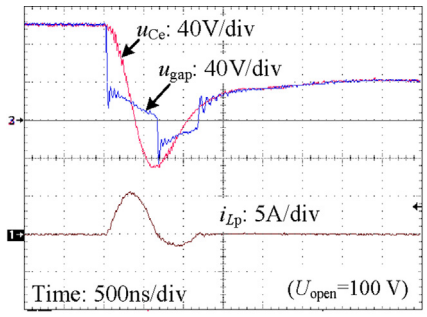

(a) Micro-EDM in deionized water on Agie®.

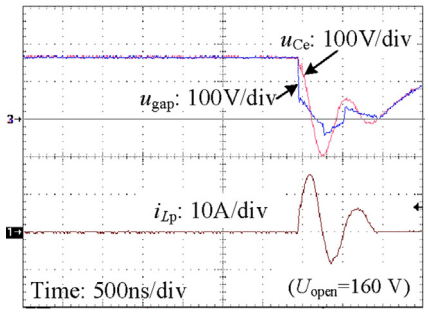

(b) Micro-EDM in oil on Sarix®.

Fig. 2. Micro-EDM sparking phenomena with negative current.

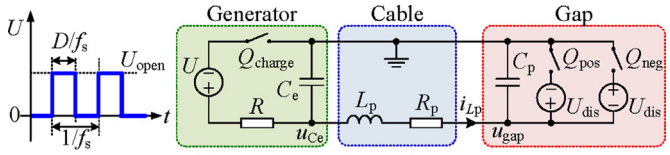

(a) Simulation electrical circuit

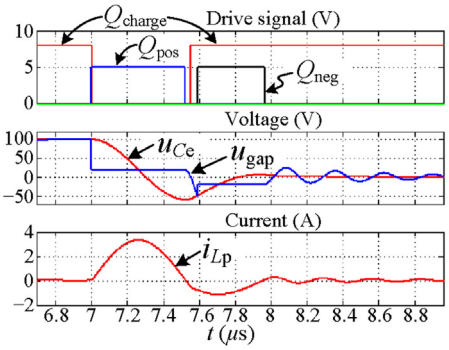

(b) Simulation waveforms

Fig. 3. Simulation circuit and waveforms.

the electrical circuit with a RC type generator used in simulation, and the sparking gap model, which includes three parts:

1. A pulse generator composed of a voltage source U controlled by a switch Q_{charge}, a resistor R, and a capacitor C_e. U provides pulse voltage with a frequency f_s and duty cycle D, and the output voltage is U_{open} in the period D/f_s and 0 during the rest of the time, this way there is only one normal breakdown arising from the set open voltage in each switching period $1/f_s$. Q_{charge} turns on and off when the gap voltage reaches U_{open} and zero, respectively, so that the charging circuit works upon the completion of the first normal discharge.
2. A connection cable that consists of a parasitic inductor L_p and a parasitic resistor R_p.
3. A discharge gap that consists of a parasitic capacitor C_p and two parallel constant voltage sources with opposite polarities. The two voltage sources represent the status of the sparking gap and are controlled by two power switches, Q_{pos} and Q_{neg}, respectively. Q_{pos} turns on with a short time delay after the gap voltage reaches the set open voltage, which simulates the ionization and the positive breakdown. It turns off when the discharge current i_{Lp} reaches zero [10]. Q_{neg} has the similar operation logic of Q_{pos} in the negative polarity, which simulates the negative discharge.

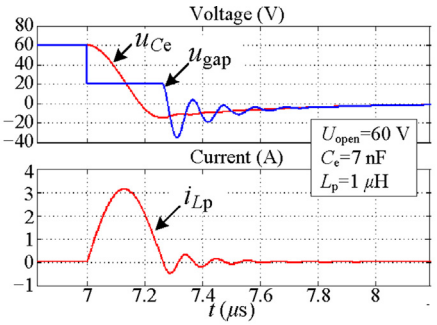

(a) Normal discharge with low U_{open}

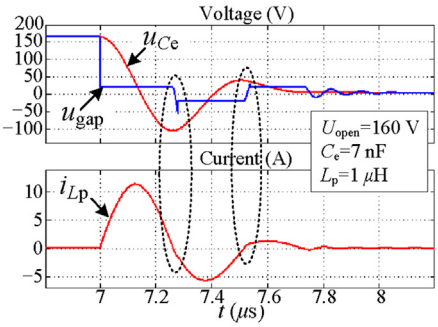

(b) Alternating discharge current with high U_{open}

Fig. 4. Simulated waveforms of u_{Ce}, u_{gap} and i_{Lp} varied with U_{open}

From the observed discharge waveforms shown in Fig. 2, the peak voltages on the gap u_{gap} for both polarities appear to beat the same level, so U_{dis} has been set at 20 V. The following open voltages u_{Ce} are relatively lower in comparison with that of the first normal discharge and are set at 50 V in the simulation. Fig. 3(b) illustrates an example simulation of the waveforms of the drive signals of the three switches (top), u_{Ce} and u_{gap} (medium) and i_{Lp} (bottom). When the drive signal is higher than 5 V or 8 V, the corresponding switch turns on.

Fig. 4 shows the simulated waveforms obtained by using Matlab® Simulink® for the normal discharge and discharge with alternating current flow under different open voltages, when R = 40 Ω, R_p = 0.06 Ω, and C_p = 500 pF (R_p, and C_p are measured values on Sarix® machine). It can be seen that the negative voltage of u_{Ce} increases along with the increase of the set open voltage. When the discharge is completed, due to the substitution of U_{dis} by C_p, the resonant time is reduced to a very low value and the waveforms vary drastically. The normal discharge waveforms in Fig. 4(a) are also similar to the experimental results. As for the alternating waveform shown in Fig. 4(b), after the first discharge, sequential gap breakdowns are imposed once the gap voltage reaches about ±50 V (dashed-lined regions) to mimic the observed sparking gap status. Since the discharge loops for both polarities share the same tank circuit (L_p and C_e), the discharge duration time is nearly the same.

It can be easily concluded by simulation and calculation that if C_e increases, the peak discharge current and discharge duration time will increase as well. When L_p increases, the peak discharge current decreases and the discharge duration time will increase. Discharges under the same product of L_p and C_e have nearly the same discharge duration time, which means that all the waveforms are influenced by L_p and C_e. The open voltage U_{open} and discharge voltage U_{dis} basically determine the peak value of the negative voltage, which affects the possibility of alternating discharge current flow.

Please cite this article in press as: Qian J, et al. Material removal mechanism in low-energy micro-EDM process. CIRP Annals - Manufacturing Technology (2015), http://dx.doi.org/10.1016/j.cirp.2015.04.040

3. Experimental investigation of alternating current flow

Further experiments have been carried out to investigate the alternating current flow phenomenon on a micro-EDM milling machine, Sarix® SX 100 HPM. Two differential voltage probes, TESTEC® TT SI9002 with a bandwidth of 25 MHz and Probe master 4233 with a bandwidth of 100 MHz, respectively, are used to acquire the generator output voltage u_{Ce} and the gap voltage u_{gap}. A current probe Tektronix® TCP312 with a bandwidth of 100 MHz is used to acquire the discharge current waveform i_{Lp} which is then transferred to a voltage signal by an amplifier Tektronix®TCPA 300. A National Instruments® data acquisition card (NI PXI-5152), with a sampling rate of up to 1 GS/s per channel, has been used to acquire the real-time waveforms of the discharge current and gap voltage used respectively for discharge pulse counting and micro-EDM pulse discrimination. The tool electrode is a 500 μm tungsten carbide rod, the workpiece is of stainless steel AISI 420 (STAVAX® ESR), and the dielectrics hydrocarbon oil (HEDMA® 111).

3.1. Experimental waveforms

Fig. 5 shows the experimental waveforms of u_{Ce}, u_{gap} and i_{Lp} varied with the discharge capacitor C_e. A higher value of energy setting E means a larger C_e, while other machine parameters are the same. All experiments are carried out using the same connection cable and consequently with the same L_p (1 μH) and R_p(0.05 Ω). In line with the analysis and simulation, it can be seen that with the same open voltage, both the discharge duration and the peak discharge current increase along with the C_e, and it is valid for both positive and negative current flow. With the same C_e, the discharge duration times are nearly the same because L_p is fixed. The higher the open voltage, the more energy will be stored in C_e after the first normal discharge, which will lead to higher probability and number of alternating discharge current flow after the first sparking breakdown.

Fig. 6 provides the experimental waveforms of u_{Ce}, u_{gap} and i_{Lp} with a longer connection cable with energy setting of E = 107. Since the larger L_p and R_p (L_p = 1.3 μH and R_p = 0.06 Ω), there is a longer discharge duration time and a lower peak current for both positive and negative current flows compared with the waveforms in Fig. 5(a) and (b).

3.2. Effects of alternating current flow on machining performance

Based on the theoretical analysis, electrical circuit simulation and experimental verifications, it appears reasonable to treat the following voltages and currents after the first discharge as

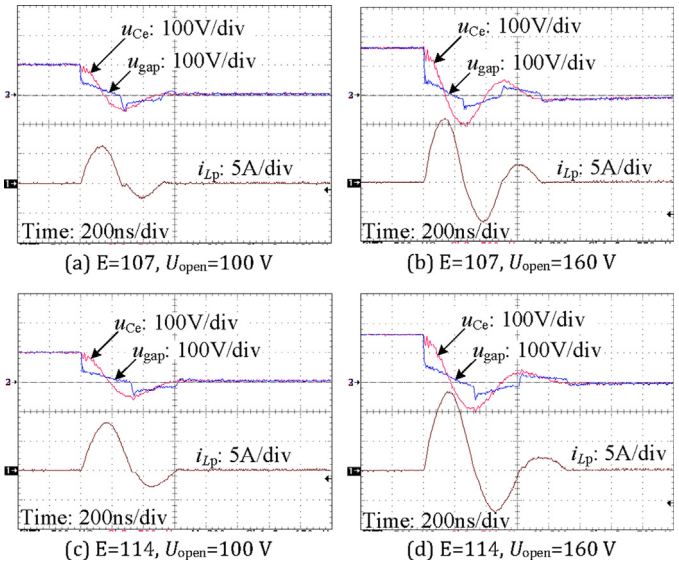

Fig. 5. Waveforms of u_{Ce}, u_{gap} and i_{Lp} varied with discharge capacitor C_e.

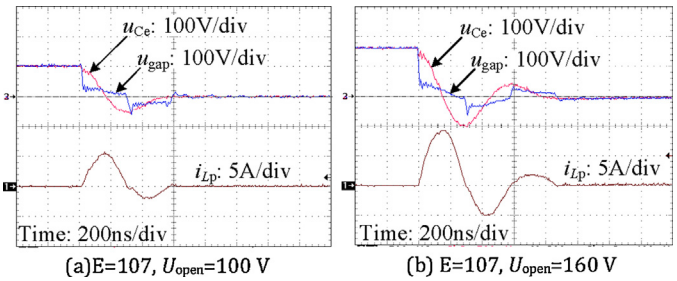

Fig. 6. Waveforms of u_{Ce}, u_{gap} and i_{Lp} with a longer connection cable.

"multi-discharges" with an open plasma channel. It is assumed that the energy consumption in the sparking gap has a dominant influence on the material removal mechanism in micro-EDM process, so it is interesting to investigate the effects of these alternating current flows. Therefore, a diode has been deliberately added into the discharge loop to prevent the alternating current phenomena and this serves as a benchmark to compare the results. As expected, with a diode in the loop, the sparking current and duration are the same as the first discharge in experiments without a diode, and the alternating current flow phenomena do not occur. All the waveforms and data acquired from the discharge circuit with an inserted diode are hereinafter called the diode case.

Circular slots of a 2 mm in diameter and a machining depth of 60 μm have been machined under different conditions, with each condition being tested 5 times and results being averaged. The method for characterizing alternating current flow is through monitoring the discharge currents with fixed current thresholds and duration time [11]. This method allows to count the positive and negative parts (pulses) of an oscillating discharge. The wear on the tool electrode, erosion time and workpiece material removal rate are calculated by the machine after the process.

As illustrated in Fig. 7, the occurrence of negative pulses increases along with the voltage u_{Ce} increase from 100 V to 120 V. From 120 V to 160 V, the positive pulse number decreases gradually and the negative pulse number also reduces but at a somewhat smaller rate. But the ratio of the negative pulse to the positive pulse increases with the open voltage and it increases to a high value especially in a high open voltage case.

When a diode is inserted into the discharge loop in series (dashed line), since there is no alternating current flow, the discharge duration time becomes short and it leads to an immediate recharge of the discharge capacitor. So the total number of discharges per unit time is higher compared to the non-diode case, although it also decreases when increasing the voltage from 120 V to 160 V.

Fig. 8(a) shows the variation of material removal per discharge (MRD) and tool wear per discharge (TWD) along with the open voltage. For the diode case, since there is only one discharge for

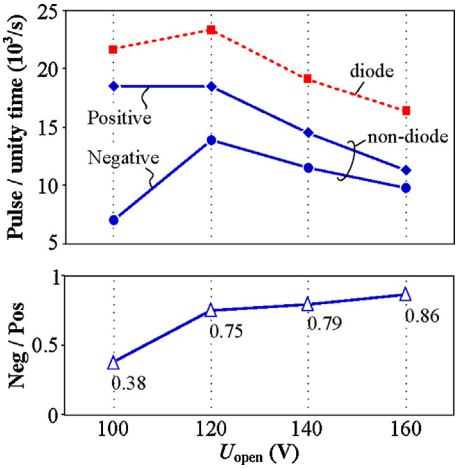

Fig. 7. Alternating pulse ratio and pulse per unity time.

Please cite this article in press as: Qian J, et al. Material removal mechanism in low-energy micro-EDM process. CIRP Annals - Manufacturing Technology (2015), http://dx.doi.org/10.1016/j.cirp.2015.04.040

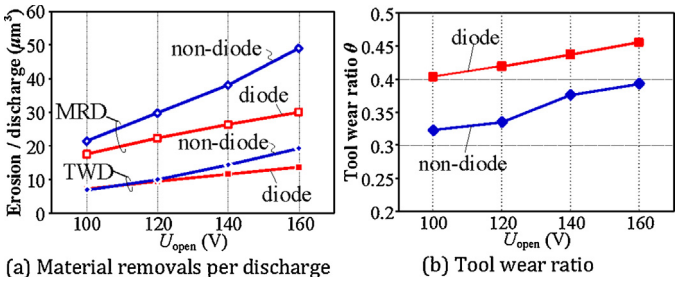

Fig. 8. Material removals per discharge and tool wear ratio in diode and non-diode cases.

each charging and the energy consumed for one discharge is proportional to the open voltage, the material removal per discharge increases in a nearly linear manner. However, for the non-diode case the material erosion per discharge for both the tool electrode and the workpiece are larger than that in the diode case, and they increase along with the open voltage. Fig. 8(b) shows the tool wear ratio (TWR) for diode and non-diode case, and it also can be treated as the ratio of tool wear and workpiece material removal in one normal gap breakdown. It clearly indicates that the TWR in non-diode case is lower than that in a diode case. In combination with the TWD and MRD in Fig. 8(a), this suggests that, in "negative polarity" micro-EDM machining, the negative current part in the alternating current flow situation is contributing to very effective material removal and it is causing less tool wear contrary to the conventional understanding. This has been further experimentally verified in an indirect way.

Fig. 9 depicts the tool wear ratio in "positive" and "negative" polarity machining. In order to eliminate the alternating current flow effects, all the tests have been carried out with a diode inserted in the loop. Obviously the TWR is smaller than 1 for "negative" polarity and higher than 1 for "positive" polarity, which is in line with the current knowledge about micro EDM [2]. If the alternating current flow would be a simple combination of discharges of different polarity, the TWR in sparking without a diode in Fig. 8(b) should be higher than that in sparking with a diode. A possible reason for this positive contribution of the negative current flow is that those heavy ions which have not reached the tool electrode within the short period of the first breakdown bombard back on the workpiece during the negative current flow. This alternating current flow also suggests that the plasma channel remains open when the sparking current reaches zero. However this needs further investigation and clarification.

The topography of the surfaces produced by micro-EDM has been examined under a SEM (FEI® XL30 FEG) and Fig. 10 shown the sparking craters obtained in both the diode and non-diode cases under different open voltages. It appears that the edges of the craters generated in the sparking with alternating discharge current flow, i.e. in non-diode case, are smoother than those left after sparking in the single discharge case with a diode inserted in the loop. It is supposed that the total energy consumption in one crater in the non-diode (discharge with alternating current flow) case is much higher than that in the diode case, so its melting/smoothing effect of the sparking is more obvious, especially with a high applied open voltage.

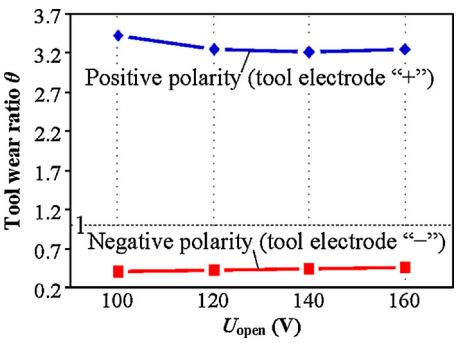

Fig. 9. Tool wear ratio in positive and negative polarity with a diode.

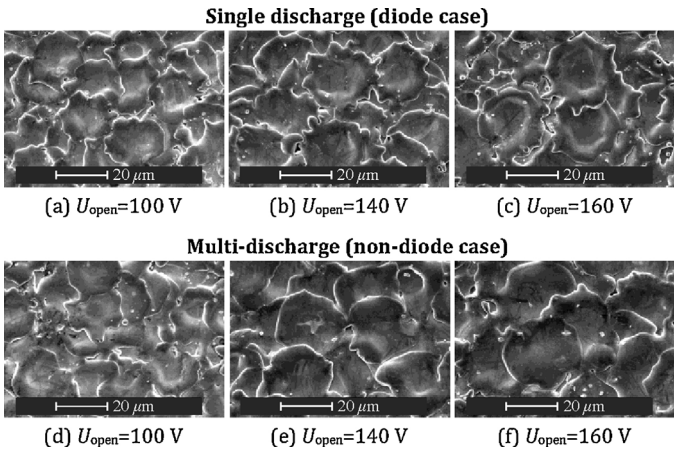

Fig. 10. SEM pictures of craters in diode and non-diode cases.

4. Conclusions

The phenomena of sparking with alternating current flow in micro-EDM process using a RC type generator have been analyzed through electrical circuit simulation and further experimentally investigated. Due to the cable inductance between the generator and the gap, there is a resonance in the discharge capacitor which leads to an alternating current flow.

Due to this alternating current flow, the material removal rate is eventually much higher compared to the sparking without the negative current flow and this makes the tool wear prediction to become more complicated.

Experimental results, obtained in negative electrode polarity mode and with settings in the low energy regime on a commercial device, indicate that the negative current flow part is effectively contributing to the material removal on the workpiece. However, further investigation is necessary to explain these results.

Acknowledgements

This research has been carried out within the framework of EC Project Hi-Micro (Grant No. 314055) and KU Leuven VES F+.

References

[1] Masuzawam T (2001) Micro-EDM. *Proceedings of the 13th International Symposium for Electromachining*, 3–19.
[2] Kunieda M, Lauwers B, Rajurkar K, Schumacher B (2005) Advancing EDM Through Fundamental Insight Into the Process. *CIRP Annals – Manufacturing Technology* 54(2):599–622.
[3] Rajurkar K, Levy G, Malshe A, Sundaram M, McGeough J, Hu X, Resnick R, De Silva A (2006) Micro and Nano Machining by Electro-Physical and Chemical Processes. *CIRP Annals – Manufacturing Technology* 55(2):643–666.
[4] Han F, Wachi S, Kunieda M (2004) Improvement of Machining Characteristics of Micro-EDM Using Transistor Type Isopulse Generator and Servo Feed Control. *Precision Engineering* 28(4):378–385.
[5] Wong Y, Rahman M, Lim H, Han H, Ravi N (2003) Investigation of Micro-EDM Material Removal Characteristics Using Single RC-Pulse Discharges. *Journal of Materials Processing Technology* 140(1–3):303–307.
[6] Egashira K, Matsugasako A, Tsuchiya H, Miyazaki M (2006) Electrical Discharge Machining With Ultralow Discharge Energy. *Precision Engineering* 30(4): 414–420.
[7] Kao C, Shih AJ (2006) Sub-Nanosecond Monitoring of Micro-Hole Electrical Discharge Machining Pulses and Modeling of Discharge Ringing. *International Journal of Machine Tools & Manufacture* 46(15):1996–2008.
[8] Tomura M, Kunieda M (2010) Study on Uncertainty of Discharge Energy in Micro EDM. *Proceedings of the 4th CIRP International Conference on High Performance Cutting*, 331–336.
[9] Braganca M, Rosa P, Dias F, Martins P, Alves L (2013) Experimental Study of Micro Electrical Discharge Machining Discharges. *Journal of Applied Physics* 113(233301):1–14.
[10] Descoeudres A (2006) *Characterization of Electrical Discharge Machining Plasmas*, (Ph.D. Dissertation) Ecole Polytechnique Federale De Lausanne, Lausanne.
[11] Wang J, Ferraris E, Galbiati M, Qian J, Reynaerts D (2014) Simultaneously Counting of Positive and Negative Pulse Parts to Predict Tool Wear in Micro-EDM Milling. *Proceedings of the 9th International Conference on Micromanufacturing*, 111.

Please cite this article in press as: Qian J, et al. Material removal mechanism in low-energy micro-EDM process. CIRP Annals - Manufacturing Technology (2015), http://dx.doi.org/10.1016/j.cirp.2015.04.040